

# Characterization of O<sup>-</sup>-centers on single crystalline MgO(001)-films

A. Gonchar<sup>1</sup>, J. Lian<sup>1</sup>, T. Risse<sup>1,3,4,\*</sup>, H.-J. Freund<sup>1</sup>, C. Di Valentin<sup>2</sup>, G. Pacchioni<sup>2</sup>,

<sup>1</sup>*Fritz-Haber-Institut der Max-Planck-Gesellschaft, Faradayweg 4-6, 14195 Berlin*

<sup>2</sup>*Dipartimento di Scienza dei Materiali, Università di Milano-Bicocca, via R. Cozzi, 55-20125, Milano, Italy*

<sup>3</sup>*Institut für Chemie und Biochemie, Freie Universität Berlin, Takustr. 3, 14195 Berlin*

<sup>4</sup>*Berlin Joined EPR Laboratory, FU Berlin and Helmholtz-Zentrum für Materialien und Energie, Berlin*

## Abstract

Defects play an important role for understanding the properties of oxide surfaces. However, a detailed atomistic characterization of the properties of defects in particular of point defects is still a challenging task. On polycrystalline material it is large variety of different species in terms of local environment as well as electronic properties as well as the metastable nature of most of these species, which complicates matters. EPR spectroscopy has proven to be a versatile tool to characterize a electronic properties as well as the local environment of paramagnetic point defects on oxide surfaces. In this study we elucidate the properties of O<sup>-</sup>-centers on MgO surfaces under ultrahigh vacuum (UHV) conditions using a single-crystalline MgO(001) surface as a well-defined model system. The O<sup>-</sup>-centers were produced by reaction of N<sub>2</sub>O with previously prepared F<sup>+</sup>-centers, which were shown to be located at step edges of the MgO islands in a previous study. The experimental efforts are combined with ab-initio quantum chemistry calculations to gain a more detailed understanding of the electronic properties of the defects under consideration. The experimental and theoretical values of the g-tensor components are almost in quantitative agreement, a degree of correlation not regularly found for the g-tensor

components of oxygen based radicals on MgO surfaces. In addition to the discussion of the properties of O<sup>-</sup>-centers the paper will shed some light on the impact that doping of the surface in this case with Mo(V)-species present on the pristine surface has. In particular, we are able to provide evidence for the fact that there is redox chemistry between the O<sup>-</sup>-centers and Mo-centers. **The crosstalk between different redox active sites on the surface is an important phenomenon that is not limited to model systems as discussed here, but should also be taken in to consideration if discussing the properties of high performance catalysts.**

Keywords: EPR spectroscopy, oxide surface, MgO, point defects, suboxide anions radical, Mo(V), doping

\*Corresponding author:

[risse@chemie.fu-berlin.de](mailto:risse@chemie.fu-berlin.de),

Tel: ++49-30-838-55313

Fax: ++49-30-838-4-55313

## 1. Introduction

The interface between oxides with gases or liquids plays an important role not only for heterogeneous catalysis but also for other various branches of technology such as sensor technology, corrosion protection, or semiconductor devices. This has served as a driving force for substantial efforts in the last decades aiming at an atomic level understanding of the properties of oxide surfaces and interfaces. It turned out that the properties of oxides depend strongly on the presence of defects, both extended and point defects, the latter including low-coordinated sites, impurity atoms, vacancies as well as electron or hole centers. Different experimental as well as theoretical methods have been used to characterize their properties in detail. However, even for simple systems such as magnesium oxide, which can be considered the prototype of an ionic oxide with a simple rock-salt structure, a detailed characterization of defects still poses a significant challenge. The difficulties arise not only by the fact that even a presumably simple defect such as an anion vacancy in MgO may be found in different local environments (e.g. located at steps, edge, kinks or terrace sites) or different charge states, but also that most of the defects are metastable minority species. To reduce the complexity encountered for polycrystalline material typically used in applications such as heterogeneous catalysis, single crystalline metal oxide surfaces –either bulk single crystals or single crystalline oxide films grown epitaxially on various conductive single crystal substrates- have been successfully used to gain insight into the atomistic details of defects on oxide surfaces [1-3]. The approach allows to apply the toolbox of surface science methods developed over the last decades as well as the investigation of the systems under well-defined ultrahigh vacuum conditions, which ensures a controllable interaction of the defect sites with the environment. An important subset of defects present on oxide surfaces is paramagnetic, which makes these centers susceptible to studies by electron paramagnetic resonance (EPR) [4]. In comparison with other spectroscopic techniques available to characterize

surface defects, EPR spectroscopy provides a very high energetic resolution. If applied to single crystalline material as done in this study, the anisotropic nature of the interaction between the unpaired electron and its environment as well as the magnetic field provides means to determine the surface sites of the species under consideration [5,6]. It has been shown that, in particular, a combination of EPR spectroscopic investigations with high level quantum chemical calculations can give additional important insight into the microscopic properties of the system [7-9].

MgO is an ideal solid to study the properties of paramagnetic defects. Apart from morphological surface defects such as edges, kinks, steps, or dislocation lines, intrinsic point defects such as cation or anion vacancies, may be present. Anion vacancies also called color centers or F-centers in the bulk of MgO and other alkaline earth oxides have been studied comprehensively in the past using EPR as well as optical spectroscopy, see e.g. [10-12,3]. A variety of studies has been published on the nature and properties of their surface analogs often called  $F_s$ -centers on powdered material [13-23]. Color centers were investigated on single crystalline MgO(100) films under ultrahigh vacuum conditions, which allows to study the centers in the absence of interaction with adsorbates from the gas-phase. Electron energy loss spectroscopy (EELS), electron paramagnetic resonance (EPR) spectroscopy as well as scanning probe microscopy (STM/AFM) and spectroscopy (STS) have been used to characterize  $F_s$  centers of single-crystalline MgO(001) thin films namely ( $F^{0-}$ ,  $F^{+-}$  and  $F^{2+-}$  centers), which were found to be preferably located on edges and corners of the MgO(001) islands [24,25,6,26]. Apart from anion vacancies also electron deficient anion centers ( $O^-$ -center) are considered to play a role in catalytic reactions. While there are numerous examples in the field of heterogeneous catalysis and in particular in photocatalytic applications, a prominent example with respect to MgO is the oxidative coupling of methane. The latter reaction was studied in detail using Li-doped MgO as a catalyst system and from these investigations a general reaction pathway was deduced, which

involves O<sup>-</sup>-centers to be responsible for the primary abstraction of a hydrogen atom from the methane molecule [27]. The O<sup>-</sup>-centers are stabilized by the introduction of low-valent Li ions into the alkaline earth lattice. Theoretical studies have shown that this low-valent doping indeed reduces the activation energy of the OCM process [28-30]. However, the applicability of this mechanism was challenged in literature, not the least by the observation that even pure MgO works as a catalyst [31-33]. Even though the stabilization of O<sup>-</sup>-centers in MgO by Li-doping is not sustainable over longer time scales under the harsh experimental conditions, the use of redox active dopants to alter and in the best case to control the reactivity of the system is an important concept. While the concept is very well known, studies that utilize this approach for high performance catalysts, with sufficient control of the system to prove the importance of the doping for the observed properties, are rather scarce. Notably, this concept has recently been shown to work nicely for the OCM process [34]. However, an atomic level characterization of the different species, as well as their interaction, is challenging on a high performance catalyst, in particular if reactive species are involved. To this end studies using model systems under well-defined conditions provide means to address such aspects. In this paper we use EPR spectroscopy under ultrahigh vacuum (UHV) conditions to characterize O<sup>-</sup>-centers on single-crystalline MgO(001)-films and elucidate their interactions with molybdenum dopants present in these films.

O<sup>-</sup>-centers on MgO surfaces have been investigated in detail using EPR spectroscopy as well as other spectroscopic techniques on high surface area, polycrystalline material [35-38,23,22,39]. Different preparation techniques were employed to produce the centers. Among those the reaction of singly charged color centers with an atomic oxygen source such as N<sub>2</sub>O according to



was shown to be a versatile strategy. A variety of different  $O^-$ -centers have been identified, whose relative abundance depend on the details of the preparation techniques. All centers described in literature on MgO are characterized by an axial g-tensor indicating a rather high local symmetry of the corresponding sites. Even though all centers exhibit an axial symmetric g-tensor, the perpendicular components of the tensor differ considerably between the centers. In a simple ligand field picture this behavior can be understood by assuming that in a ligand field of high enough symmetry the two doubly occupied p-orbitals of the  $O^-$ -centers are degenerate and energetically separated from the single occupied orbital usually denoted as the  $p_z$ -orbital. Within the ligand field model this situation leads to an axial symmetric g-tensor with tensor components given by

$$g_{||} \approx g_e \quad (2)$$

$$g_{||} \approx g_e + \frac{2\lambda}{\delta E} \quad (3)$$

where  $\lambda$  denotes the spin-orbit coupling constant and  $\delta E$  is the energy difference between the ground state and the first excited state of the system. In case of a lower symmetry the degeneracy of the two doubly occupied p-orbitals is lifted resulting in an orthorhombic g-tensor whose value depend additionally on the energy difference between the split  $p_x$  and  $p_y$  orbitals [40].

EPR investigations on  $F^+$ -centers on single crystalline MgO(001)-films have shown these centers to be predominately located at step sites of the MgO islands [6]. If using these sites as the starting point to create  $O^-$ -centers according to equation (1), hence creating suboxide anions at step edges a lifting of the typically observed axial g-tensor into an orthorhombic one is expected. Since the spin-orbit coupling of an unpaired electron located in a p-orbital of an oxygen ion is much larger than that of the electron being located in the Madelung potential of the surrounding cations the

spectral resolution of the angular dependent spectra is expected to significantly enhanced for the  $O^-$ -centers, which may allow to confirm the previous assignment based on the analysis of the  $F^+$ -centers.

The paper is organized as follows: after giving some details on the experimental and theoretical methods we will start by briefly reviewing the main properties of  $F^+$ - as well as  $Mo(V)$ -centers on  $MgO(001)$  films grown on  $Mo(001)$ . The discussion of the  $Mo$ -centers, which at first glance seems to be unrelated to the main topic of the paper, will turn out to be important to understand the chemical properties of the system. The body of the result part will be devoted to the reactivity of the  $F^+$ -centers with  $N_2O$ , which is considered to fill oxygen vacancies as schematically indicated in scheme 1 above. In case of a singly occupied vacancy ( $F^+$ -center) this reaction should result in an  $O^-$ -center, whose properties will be characterized by EPR spectroscopy. However, the EPR results also show that additional chemical processes involving  $Mo$ -centers take place on the surface. The advantage of using a single crystalline sample is the ability to determine not only information on the principal components of the  $g$ -tensor but also on the orientation of the  $g$ -tensor with respect to the surface from angular dependent measurements. In particular, in light of the large body of data available from  $MgO$  powders it is important to compare the observed experimental results with theoretical calculations to validate the analysis of the experimental results and to benchmark the accuracy of current theory on a well-defined model system.

## **2. Experimental and theoretical methods**

Experimental methods

Experiments were carried out in an UHV chamber equipped with standard facilities for thin film preparation and characterization, which has been described in detail elsewhere [41]. The base pressure of the system was  $2 \times 10^{-10}$  mbar and well below  $1 \times 10^{-10}$  mbar during the EPR measurements. The preparation of the substrate and the films follows recipes described in literature [42]. In short the Mo(100) substrate was cleaned by oxidation at 1500 K in  $1 \times 10^{-6}$  mbar  $O_2$  and subsequent annealing to 2300 K. For the preparation of the MgO films Mg was evaporated onto the clean Mo single crystal surface in an oxygen background pressure of  $2 \times 10^{-6}$  mbar at a rate of approximately 1ML/min and a substrate temperature of 600 K. The formation of a crystalline MgO(100) film was verified using low energy electron diffraction (LEED). EPR measurements were performed at 30 K (unless otherwise stated) and a microwave frequency of  $\sim 9.67$  GHz (X-band) using a  $TE_{102}$  resonator. A microwave power of 2 mW and a modulation amplitude of 0.4 mT were used, which avoids saturation or overmodulation effects. The spectra presented here were carefully background corrected. The g-values given here were calibrated against DPPH ( $g = 2.0036$ ). Surface color centers were electrons from a filament with a fixed energy of 100 eV. The electron dose was in the range of 200 – 500 e-/surface  $O^{2-}$  ion, which is range of does to create the maximal number paramagnetic  $F^+$ -centers on the surface [43]. Simulations of the EPR spectra were done using the easyspin package [44].

## **Theoretical methods**

The spin properties of single trapped holes at low coordinated sites of the MgO surface have been computed by electronic structure calculations on quantum chemical embedded cluster models with the Gaussian09 code [45]. The calculations have been performed at the DFT level using the gradient corrected Becke's three parameters hybrid exchange functional [46] in combination with



the correlation functional of Lee, Yang and Parr [47]. The quantum chemical (QM) part of the clusters is embedded in an array of about 8000 point charges. The interface between the QM cluster and the point charges includes Mg ions which are represented by semi-local effective core potential (ECP) [48] to prevent an artificial polarization of the oxygen anions in the QM cluster. QM atoms have been fully relaxed. Three clusters have been used to model the corner  $[\text{Mg}_{10}\text{O}_{10}]_{\text{corner}}$ , the edge  $[\text{Mg}_{10}\text{O}_{10}]_{\text{edge}}$  and the step edge  $[\text{Mg}_{11}\text{O}_{11}]_{\text{steo}}$  on the MgO surface. A 6-31 G basis set on all Mg and O ions [49,50] has been used for geometry optimization, while the g-tensor components have been obtained performing single point calculations on the optimized geometries using a more flexible basis set, with 6-311+G\* on Mg and EPR-II on O [51]. For the determination of the g-tensors we used the spin-orbit perturbation strategy in the scheme proposed by Neese [52] and implemented in the Gaussian09 code.

### 3. Results and Discussion

Figure 1a-c shows the angular dependent EPR spectra taken at  $90^\circ$ ,  $30^\circ$ , and  $0^\circ$  with respect to the surface normal which were observed after bombarding a pristine, 20 ML thick MgO(001) film[6]. The spectra were recorded at 300 K using a modulation amplitude of 0.1 mT to avoid broadening of the lines. The spectra are found at g-values very close to the g-value of the free electron, hence, the centers can be assigned to paramagnetic color centers ( $\text{F}^+$ -centers) of the MgO(001) film, which in contrast to paramagnetic oxygen centers of MgO show only very small deviations from the g-value of the free electron (e.g. [53,11,54,55,18,56,57]). As EPR spectroscopy is not a surface sensitive technique it is important to investigate if the centers are located on the surface of the film or in its bulk. This information is readily available by interacting the color centers e.g. with gases or other adsorbates. To this end it has been shown using Au as an exploratory example that the EPR signal of the paramagnetic color centers is

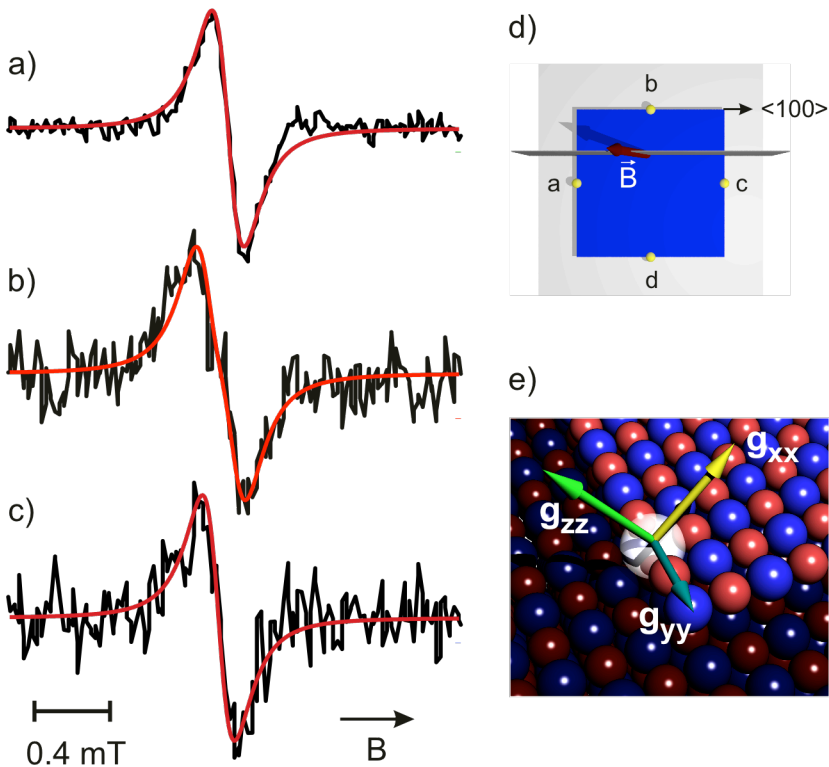


Figure 1: a-c) EPR spectra taken at 300 K of a 20 ML thick MgO-film after electron bombardment spectra are taken at an angle of  $90^\circ$  (a),  $30^\circ$  (b) and  $0^\circ$  (c) with respect to the surface normal. d) geometric relation between the edges of the MgO islands (oriented along  $\langle 100 \rangle$  equivalent directions) and the orientation of the plane in which the magnetic field can be rotated. a, b, c, d indicate symmetry equivalent sites on the MgO surface. e) schematic view of the g-tensor orientation for a  $F^+$ -center located at the edge of a MgO island.

readily quenched by deposition of metal atoms or particles. The deposition of Au particles onto the color centers results in a charge transfer of the electron residing in the color center to the Au atoms and particles [5,58]. The location on the surface of the MgO(001) film is in line with the observation that the measured spectra show a small but significant angular dependence, which would not be expected in the bulk of MgO because of the high symmetry of the rock salt lattice. The angular dependence of the line shape is due to the g-tensor anisotropy of the surface color centers. Understanding the line shape requires knowledge not only on the g-tensor components but also on the orientation of the tensor with respect to the surface. An analysis of the angular

dependent line shape allows to assign the spectra to color centers located at edge sites of the MgO islands. More precisely speaking it is possible to discriminate between sites having two principal tensor components in the (110)-plane (such as corner sites) and sites, which have the g-tensor components in (100) equivalent planes. The latter is expected for color centers located at edges of the MgO islands. Figure 1e shows schematically the orientation of the g-tensor expected for a color center located at a step edge of the MgO islands. While symmetry arguments require one principal tensor component to be oriented along the step edge, the orientation of the other two tensor components is not determined by symmetry in contrast to the situation on a MgO cube found in high quality MgO powder, where the color center at the edge of the cube exhibits a  $C_{2v}$ -axis inclined  $45^\circ$  to both adjacent (100)-type faces of the cube. For this situation one of the g-tensor components has to be aligned with the  $C_{2v}$ -axis. It is important to realize that on a MgO island, having edges running along  $\langle 100 \rangle$  equivalent directions [59,60], four symmetry equivalent edges exist as indicated in Figure 1d). Applying a magnetic field lifts the degeneracy of the edges. If the magnetic field is rotated in a plane containing the surface normal and a  $\langle 100 \rangle$  equivalent direction it is expected that two different signals are observed for the magnetic field aligned in the surface, only one signal contributes to the spectrum in normal incidence, and three signals are present for all other orientations of the magnetic field given the second tensor component is not oriented along the surface normal as indicated in Figure 1e. This is exactly what is found in the spectra showing the smallest line width at normal incidence and the broadest signals for orientations between  $0^\circ$  and  $90^\circ$ . From these arguments it is possible to assign the observed signal to color centers located at the edges of the MgO islands. It is important to note, that the resolution of the data is insufficient to exclude the presence of a minority of color centers located at corners of the MgO islands. The latter have been observed by combined STM/STS studies and are expected to be present based on the relative formation energy of color centers on

edge as compared to corner sites [25,61-64]. Information on g-tensor components as well as the orientation of the g-tensor with respect to the site of interest comes from theoretical investigations. To this end theory shows that going from the edge of a cube with one principal component of the g-tensor aligned with the  $C_{2v}$ -axis to a monoatomic step results in a rotation of the g-tensor around the axis defined by the step edge by about  $20^\circ$  [65]. With this constrain slightly different g-tensor components are found after fitting the experimental data to yield:  $g_{xx} = 1.999\ 95$   $g_{yy} = 2.000\ 09$   $g_{zz} = 2.000\ 24$ . While the anisotropy of the values can be determined quite accurately, the absolute value of the isotropic part of the g-tensor is to the best as good as the DPPH reference ( $g = 2.0036$ ) used to calibrate the field. It may be noted in passing that the theoretical calculations clearly show that the g-tensors of the color centers are probing only a very small area around the center namely the nearest neighbor O and Mg ions. The location of more distant ions as well as the details of the Madelung potential are playing only a minor role.

An important question that remains unaddressed when discussing the properties of paramagnetic color centers created by electron bombardment concerns the stability of these centers as they represent charge imbalances as compared to the stoichiometric lattice. To account for the Coulomb repulsion of the centers it is necessary to compensate the charge imbalance in the film. The question arises how this charge compensation takes place in the single crystalline MgO(001)-film discussed here. To this end it is important to note that the MgO-film grown under the given conditions exhibits Mo(V)-centers. These centers are located at the surface of the MgO(001) film as was shown by the reversible shift of the line upon adsorption and desorption of weakly adsorbing molecules such as methane. **The detailed EPR characterization of these centers has been published elsewhere [66].** Figure 2a shows the spectrum of a pristine, 20 ML thick MgO(001)-film. The Mo(V)-centers found at high magnetic field is characterized by a g-value in the surface plane of  $g_{\perp} = 1.9296$ . Symmetric to the central line six additional lines are found,

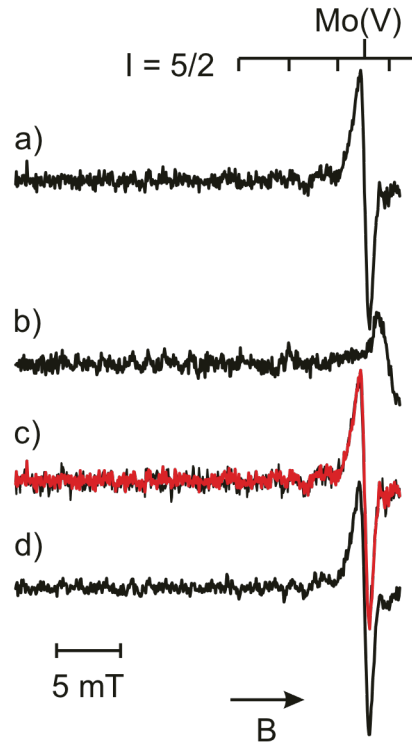


Figure 2: a) EPR spectrum of a 20 ML thick, pristine MgO-film. b) EPR spectrum after adsorption of 1.8 L N<sub>2</sub>O (1 L = 1 torr s). c) spectrum after heating the sample of b) to 160 K. The red trace is the spectrum a) overlaid. d) after heating the sample of c) to 300 K. All spectra are taken with the magnetic field oriented in the film surface and at a temperature of 30 K.

which are due to hyperfine coupling ( $A_{\perp} = 108$  MHz) of the unpaired electron with the nuclear spin of the two isotopes <sup>95</sup>Mo and <sup>97</sup>Mo with a natural abundance of 15.9% and 9.5%, respectively, both having a nuclear spin of 5/2 [66]. In Figure 2a the two high field components of the expected six hyperfine lines are clipped due to an improper choice of the field range.

Further below we want to discuss the properties of O<sup>-</sup>-centers being created by the reaction of paramagnetic color centers with N<sub>2</sub>O as an oxygen source. To allow for conclusive statements it is important to ensure that N<sub>2</sub>O does not react with the pristine MgO(001) surface to create paramagnetic species. Figure 2b shows the EPR spectrum obtained after adsorption of N<sub>2</sub>O at 30 K onto the pristine MgO surface. Upon adsorption of N<sub>2</sub>O the entire Mo(V)-signal is shifted to higher fields by about 2 mT. Concomitantly, the line width of the signal increases significantly

resulting in a decrease of the signal amplitude. It is important to verify that the observed shift is not due to a reaction of Mo(V)-centers with N<sub>2</sub>O, but rather due to adsorption of N<sub>2</sub>O molecules on the MgO surface. It is known from temperature programmed desorption (TPD) and infrared (IR) studies, that N<sub>2</sub>O desorbs molecularly from the pristine MgO(001) surface below 160 K, which correspond to adsorption energies below 0.4 eV [67]. The EPR spectrum obtained after heating to 160 K as well as one obtained after subsequent heating to 300 K are shown in Figure 2c and d, respectively. The Mo(V)-signal of the pristine film is restored already after heating to 160 K as seen by the spectrum of the pristine film overlaid in red on top of the signal measured after annealing to 160 K (black trace) and is not changing if the system is annealed to 300 K. The result shows that N<sub>2</sub>O interacts reversibly with the Mo(V)-centers present on the MgO(001) surface. From the desorption temperature the interaction of N<sub>2</sub>O with the Mo(V)-centers would be characterized as physisorption. This is in contrast to observations on molybdenum doped silica powder. For these systems a stable adsorption complex was found at 300 K assigned to N<sub>2</sub>O coordinated to tetracoordinated Mo(V)-species [68]. The latter complex decomposes at 373 K to create an O<sup>-</sup>-center, a diamagnetic Mo(VI)-center and a nitrogen molecule desorbing from the surface. Apart from the strongly different stability of the adsorption complex and the different chemistry the corresponding complexes differ in terms of their EPR characteristics. While the EPR lines are shifted to higher g-values on the silica material, a shift to lower g-values is observed for the present case, which is in line with the conclusion based on the thermal stability, that the binding situation of the N<sub>2</sub>O molecules is very different in both cases. Please note that small adsorption energies do not necessarily imply negligible impact on the electronic structure. To this end the sizable shift of the g-value observed upon N<sub>2</sub>O adsorption indicates that the electronic structure of the Mo ions is altered.

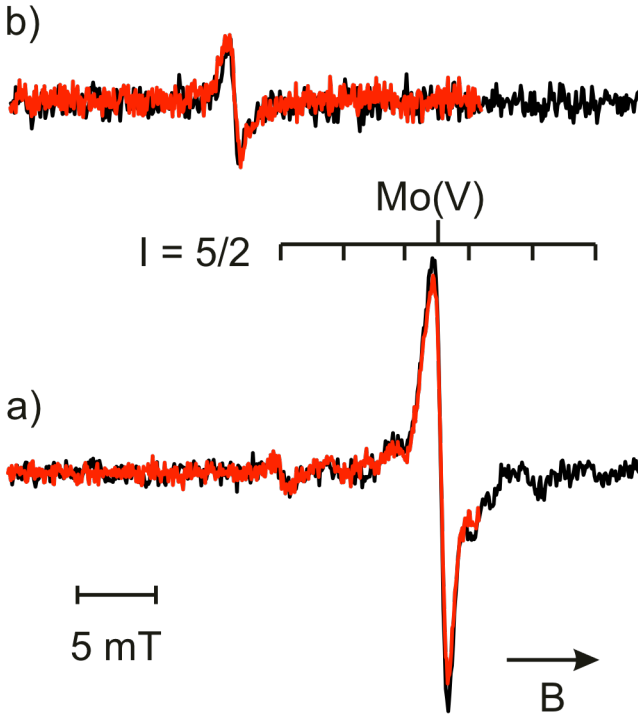


Figure 3: a) EPR spectra taken at 30 K of two 20 ML thick, pristine MgO(001) films. b) EPR spectra after exposing both films to about 200 e<sup>-</sup>/O ion.

Figure 3 shows the influence of electron bombardment on the EPR spectra of two different preparations of pristine, 20 ML thick MgO films (Figure 3a). Upon exposure of the film to about 200 e<sup>-</sup>/surface O<sup>2-</sup> ion, the well-known signal of surface color centers close to the g-value of the free electron is found (Figure 3b). Concomitantly the signal of the Mo(V)-centers vanishes indicating that electron bombardment not only creates surface F<sup>+</sup>-centers, but does also invoke redox chemistry of the Mo(V)-centers. From the signals in Figure 3a is seen that the absolute amount of Mo(V) signals on the surface is very reproducible for different preparations. For the same crystal the absolute intensity is found to vary by about 10 % between preparations. However, much larger variations are found if different crystals are compared to each other. The same holds for the number of color centers produced by electron bombardment. As seen from the spectra in Figure 3b also the intensity of the color center signal is very similar and within the

accuracy of the measurement no difference can be found for the two preparations shown in Figure 3b). It should be noted that the accuracy of the latter intensity determination is more complicated because of background signals present in the quartz finger used to seal the sample in UHV from the environment during an EPR experiment.

Electron bombardment is typically associated with a reductive environment, which would result in Mo-centers of lower formal oxidation state such as Mo(IV) or even lower. The ability of the Mo-centers to accept at least one electron can be verified by exposing the pristine surface to electron donors such as alkaline metal atoms (e.g. Li) or hydrogen atoms (data not shown). In both cases exposure of the surface to the electron donors results in a loss of the Mo(V) signal indicating the ability of the Mo(V) species to be reduced by an electron source. In turn, it is

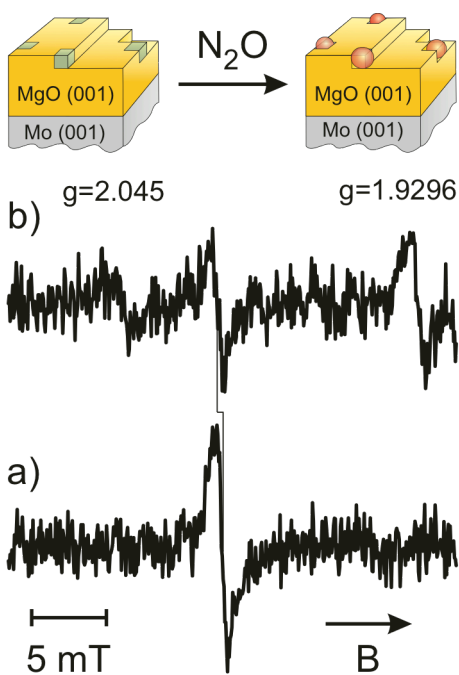


Figure 4: a) EPR spectrum of a 20 ML MgO(001)-film after electron bombardment taken at 30 K. b) EPR spectrum after adsorption of 20 L  $N_2O$  at 30 K and subsequent annealing to 160 K. Top: schematic view of the reaction between surface F-centers and  $N_2O$



expected that electron bombardment leads to a reduction of the Mo(V) species presumably to Mo(IV) or even M(III)-species. The ability of the Mo centers to become reduced upon electron exposure provides an explanation for the abovementioned issue of the charge balance within the MgO film associated to the formation of  $F^+$ -centers. To this end it is, however, important to note that the signal intensity of the Mo(V)-species found on the pristine film is about 5 times higher than that of the paramagnetic color centers after electron bombardment. Even though the precise value of the ratio has a large error, because of the ambiguities in the determination of the doubly integrated spectra associated with its background correction, the considerably larger intensity of the Mo(V) species is directly seen by inspecting the spectra. This observation directly implies that the electron bombardment of the surface induces a significant amount of additional redox chemistry in the surface and the bulk of the film, which results in species not susceptible to EPR spectroscopy.

Figure 4a shows the EPR spectrum of the electron-bombarded sample (preparation shown in Figure 3b (red trace)) as well as the spectrum after dosing 20 L  $N_2O$  at 30 K and subsequent desorption of the weakly adsorbing molecules by annealing the system to 160 K (Figure 4b). In comparison to the single line of the electron-bombarded sample,  $N_2O$  admission to these centers creates a new signal at a g-value of 2.045. In addition, the signal at around the free electron g-value decreases significantly in intensity and shifts slightly to higher g-values by  $\Delta g \approx 0.0025$ . Furthermore a signal is observed at the position of the Mo(V) centers observed on the pristine film. The transformation of the color center signal already takes place at temperatures around 50 K indicating that the corresponding process does not have a significant activation barrier. As depicted at the top of Figure 4 it is expected that surface color centers react with  $N_2O$  molecules by transferring an oxygen atom to the color center. The  $N_2$  molecule resulting as a side product of this reaction is not shown in Figure 4 for sake of clarity. The energy gain involved in the transfer

of an oxygen atom into an  $F^+$ -center through the reaction (1) was calculated to be -254 kJ/mol for an  $F^+$ -center located at a step edge [39]. The exothermicity of the reaction shows that the energy gain of filling the color center largely overcompensates the dissociation energy of the  $N_2O$  molecule being 167 kJ/mol [69]. Please note that the corresponding reaction of  $N_2O$  with diamagnetic  $F^0$ -centers containing two electrons in the oxygen vacancy, which were shown by STM/STS to be produced by the electron bombardment too, restores the stoichiometric surface. Suboxide anions on the surface of MgO have been extensively studied for powder materials (e.g. [35-38,23,22,39]). In these studies axially symmetric g-tensors with a parallel component slightly below the free electron value and two degenerate perpendicular components at higher g-values were found as listed on Table 1. In particular the perpendicular component of the g-tensor shows a strong dependence on the adsorption site of the radical and a variety of species with distinctly different values of the perpendicular component were identified. The dependence of the perpendicular component on the geometric position of the  $O^-$ -center can be understood by its dependence on the energetic splitting between ground and first excited state as described in the introduction (s. equation 1). While the picture provided by ligand field theory is useful for qualitative arguments a more quantitative comparison of different sites with similar local environments is challenging. To this end a combination of experiments with ab-initio theoretical calculations has proven to be very useful to assign the observed spectroscopic fingerprints to morphological sites of the MgO surface [70,39,71].

MgO powder	$g_{\parallel}$	$g_{\perp}$
[38,23]	2.0016	2.046
[38,23,39]	2.0016	2.0350

[23]	2.0016	2.0234
[37,38]	2.0013	2.042

Table 1: g-tensor components observed for O<sup>-</sup>-center on the surface of MgO powder. The signals are consistently characterized by an axial g-tensor.

From the data compiled in Table 1 it can be concluded that the resonance positions corresponding to g-values above  $g = 2$  observed for the single crystalline films are consistent with O<sup>-</sup>-centers on MgO surfaces. It is important to further substantiate the interpretation that the signals found at  $g > 2$  belong to the same species. To provide experimental evidence for this interpretation, the thermal behavior of these signals have been studied. Figure 5 a) shows the spectrum for a 20 ML MgO film after electron bombardment and reaction with N<sub>2</sub>O and subsequent annealing to 160 K corresponding to the spectrum observed in Figure 4b). The red trace is a fit to the data whose details will be discussed below. At present it is only used to determine the relative intensity of the signal throughout the temperature series. Figure 5b) shows the system after annealing to 300 K. The most prominent difference between the two spectra is the occurrence of a new signal at  $g = 1.985$ . The intensity of this signal is about 4 times higher than that of the two signals with  $g > 2$ . For the preceding discussion it is important to note that the signal intensity of the two signals above  $g = 2$  drops by approximately 20 % as compared to the situation in a). More importantly, both signals decrease equally. If the system is annealed to 450 K as shown in trace c) of Figure 5 the signal at  $g = 1.985$  is unchanged both in position and intensity. The low field signals drop in intensity to about half the value found at 300 K. Again, within experimental accuracy both signals with  $g > 2$  behave the same. Hence, it is concluded

that these signals belong to the same species and are assigned to  $O^-$ -centers located on the step edges of the MgO islands.

The intensity of the signals assigned to  $O^-$ -centers is always found to be smaller than the intensity of the color center signal observed prior to the adsorption of  $N_2O$  indicating that the reaction of the paramagnetic color centers with  $N_2O$  does not quantitatively result in the formation of  $O^-$ -centers. For the preparation shown in Figure 4 the reduction is 30-40 % being a typical value. It is interesting to note that within experimental uncertainty the difference between the signal intensity of the color centers and the signals with  $g > 2$  after reaction with  $N_2O$  is equal to the signal intensity of the Mo(V) species formed concomitant to the reaction of the color centers with  $N_2O$ . The correlation between the observed intensities suggests that filling the color centers with an oxygen atom is followed by a second process that restores the Mo(V) signal and decreases the

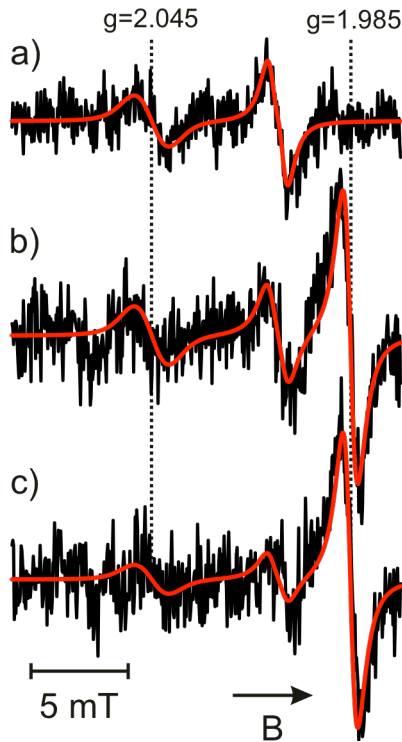
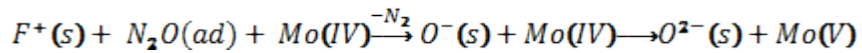


Figure 5: a) EPR spectrum of a 20 ML MgO(001)-film after electron bombardment and subsequent adsorption of  $N_2O$  at 30 K and annealing to 160 K. b) annealing of the sample in a) to 300 K. c) annealing to 450 K. All spectra are taken at 30 K.

signal of O<sup>-</sup>-centers. A likely explanation is the possibility that an electron is transferred from a closed by Mo ion. Formally this reaction may be written as:



This reaction would restore the stoichiometric edge site present prior to the electron bombardment as well as the Mo(V) signal and assumes that the electron bombardment creates Mo(IV)-centers out of the observed Mo(V)-centers present on the pristine film, which is a reasonable assumption as discussed above. Please note that the color center signal without adsorption of N<sub>2</sub>O is stable beyond 300 K, which is the temperature of the sample during the preparation of the color centers. Hence, a thermally activated charge transfer process of an electron from a reduced Mo-center to the F<sup>+</sup>-center can be excluded. The observed reaction provides yet another example for the impact of transition metal doping on the surface chemistry. To this end the use of single crystalline model systems under well-defined conditions allows us to reveal information on the participating species at the atomic level. The recent literature provides numerous examples, which illustrate the importance of doping for different aspects of the surface chemistry of oxides both from a theoretical as well as an experimental point of view (e.g. [72,34,73,74]).

The prominent signal found at  $g = 1.985$  after annealing to 300 K has an intensity which is more than 3 times larger than the intensity of the initial color center signal. In turn, this signal accounts for more than 60 % of the Mo(V) signal on the pristine film. It is important to note that this signal is only observed if the electron-bombarded surface is exposed to an oxygen atom source such as N<sub>2</sub>O. The signal is stable up to about 600 K. However, the signal disappears after annealing to higher temperatures and the original Mo(V) signal at  $g = 1.9296$  is largely restored (data not shown). Based on its  $g$ -value, which is well below the  $g$ -value of the free electron this signal is assigned to a Mo(V)-species, whose local coordination is, however, different than the one found

for Mo(V)-species on the pristine film. The latter interpretation is further corroborated by the observation that the Mo(V)-signal of the pristine film can be restored at the expense of the species at elevated temperature. This behavior underpins the abovementioned statement that complex redox chemistry involving Mo ions is taking place during bombardment with electrons and subsequent chemical and thermal treatment of the MgO surface. The details of these

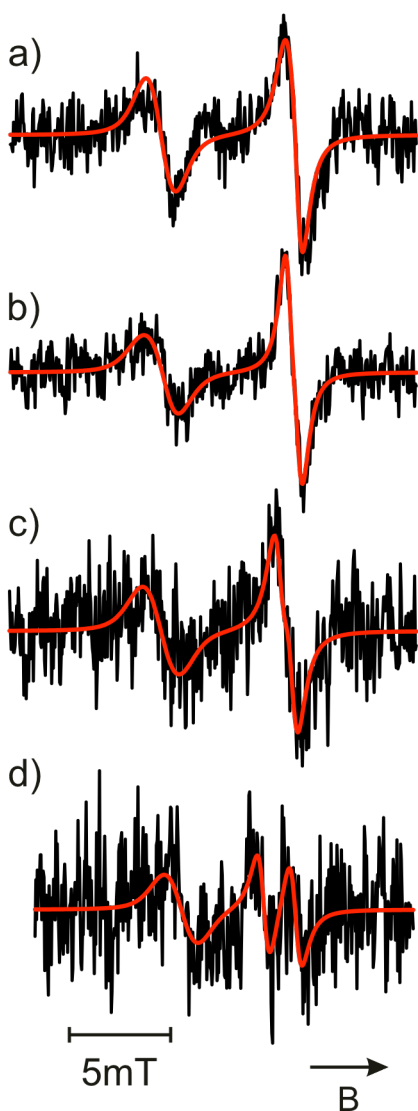


Figure 6: angular dependent EPR spectra of  $O^-$ -centers taken at 30 K. The spectra were taken with polar angle between surface normal and magnetic field at  $90^\circ$ ,  $80^\circ$ ,  $70^\circ$ , and  $60^\circ$  for trace a), b), c) and d), respectively. The magnetic field is found in a plane spanned by the surface normal and a  $\langle 100 \rangle$ -equivalent direction of the MgO(001) film.

processes are, however, beyond the scope of this article and will be discussed in a separate publication.

A comparison of the signals assigned to  $O^-$ -centers with corresponding species on MgO powder requires a detailed analysis of the spectra in terms of the principal g-tensor components. For a single crystalline sample the analysis of the data also requires knowledge of the orientation of the tensor with respect to the species at hand. The latter can be deduced from angular dependent measurements. Figure 6 shows EPR spectra taken with a polar orientation of the magnetic field of  $90^\circ$ ,  $80^\circ$ ,  $70^\circ$  and  $60^\circ$  with respect to the surface normal and an azimuthal orientation in the surface plane aligned along a  $\langle 100 \rangle$  equivalent direction. The  $O^-$ -centers discussed here are expected to be located on the edges of the MgO islands due to the location of the color centers used to create them. As these edges were shown to run along  $\langle 100 \rangle$  equivalent directions of the MgO lattice, it is possible to restrict the orientation of g-tensor [59,60]. The situation is equivalent to the one discussed for the color centers above and visualized in Figure 1. In brief, one of the principal tensor components has to be oriented along the step edge, while the other two, have to be oriented in the plane perpendicular to it, however, nothing else can be said about their orientation based on symmetry arguments. For the analysis of the data it is important to keep in mind, that MgO islands exhibit four, structurally symmetry equivalent step edges (s. Figure 1d). Applying a magnetic field lifts this degeneracy and three different situations have to be discriminated. As long as one of the principal components is not oriented along the surface normal and all components have different values, two signals with equal intensity are expected for the magnetic field oriented in the surface, while only one is expected for normal orientation of the magnetic field. For all other orientations of the magnetic field three different components are expected, which have an intensity ratio of 1:1:2 due to the fact that the two step edges parallel to

the plane in which the magnetic field can be rotated are equivalent. In addition to the measured spectra (black lines) Figure 6 also contains fits to spectra assuming the model described above.

As seen in Figure 6, an  $O^-$ -center located at step edges of the MgO islands is capable to describe the measured spectra nicely. The fits presented in Figure 6 assume a g-tensor with principal components listed in Table 2. The largest g-value of 2.045 ( $g_{zz}$ ) was oriented along the step edge while the smallest one ( $g_{xx}$ ) close to the free electron value was rotated  $15^\circ$  out of the surface plane. Correspondingly, the third component is rotated by  $15^\circ$  away from the surface normal. In order to fit the broad low field component associated with the  $g_{zz}$  component of the g-tensor properly it is necessary to assume a distribution of  $g_{zz}$  values.

For the present fit so-called g-strain implemented in the easyspin package, which assumes a Gaussian distribution of g-values around the central value, was used to account for this broadening and a full width at half maximum value of the Gaussian distribution of 0.005 was used for the gstrain of  $g_{zz}$  component. The rotation of the g-tensor in the plane perpendicular to the step edge can be determined to a few degrees, because of the observed broadening ( $70^\circ$ ) and splitting ( $60^\circ$ ) of the high field line.

It should be noted that the spectrum taken at an angle of  $90^\circ$  with respect to the surface normal has an additional line at a g-value of 2.027. This signal cannot be described by  $O^-$ -centers located at the step edges of the MgO islands. The intensity of this signal is found to vary for different preparations. In particular, higher electron dose tends to increase the intensity of this line with respect to the signals of the  $O^-$ -centers located at the edges of the islands. The position of the line is consistent with  $O^-$ -centers for which two components of the tensor are lying in a plane spanned by the surface normal and a  $\langle 110 \rangle$  equivalent direction, which is expected for corner sites or its reversed counterpart. In turn only one signal is expected for the magnetic field oriented in the surface plane. The signal intensity of this line is between 15 – 20% of the  $O^-$ -center signals



located on the edges and hence well in line with the results of structural investigations as well as the analysis of the  $F^+$ -centers [6]. A more detailed analysis of the data is hampered by the low signal to noise ratio of the spectra measured at higher angles rendering an identification of corresponding signal impossible.

In comparison to the g-tensor components observed on MgO powder (s. Table 1) the values deduced on the thin film show a significant deviation from axial symmetry. From the lack of species with non-axial symmetry it is concluded that color centers located at step edges are not found on the surface of MgO powder in larger quantities. The large deviation from the axial symmetry also implies that the reduced symmetry of the site has significant impact on the electronic structure. In particular, the degeneracy of the  $p_x$  and  $p_y$  orbitals expected for a high symmetry environment is lifted, which in turn lifts the axial symmetry of the g-tensor. While the qualitative impact of this change of local environment is readily clear, a more quantitative evaluation is difficult. To this end it is interesting to compare the experimental values with the results from theoretical calculations.

	$g_{xx}$	$g_{yy}$	$g_{zz}$
20 ML MgO(001) film	2.0035	2.025	2.045
theory			
Corner of a cube	2.0033	2.0235	
Edge on a cube	2.0050	2.0338	2.0597
Edge on a monoatomic step	2.0050	2.0236	2.0460

Table 2: g-tensor components observed for  $O^-$ -centers on a 20 ML MgO(001)-films as well as theoretical predictions of the g-tensor for different morphological sites.

Table 2 contains the principal components of the g-tensor calculated for different local geometries of  $O^-$ -centers. In line with expectations, an  $O^-$ -center located at the corner of a MgO cube exhibits an axially symmetric tensor with the g-tensor component close to the free electron value being oriented along the  $C_{3v}$ -axis (the diagonal of the cube, see right side of Figure 7). When going from a corner site of the cube to an edge site, the degeneracy of the two large g-tensor components is lifted resulting in a large value being oriented along the step edge ( $g_{zz}$ ), the principal component close to the free electron value being along the  $C_{2v}$ -axis of the edge ( $g_{xx}$ ) and an intermediate value perpendicular to the other two ( $g_{yy}$ ), see the middle panel of Figure 7. It is important to note that both the  $g_{yy}$  and the  $g_{zz}$  component of the edge center of a cube are larger than the perpendicular component found for the corner site, which is in line with qualitative arguments concerning the electronic structure, which would suggest that a lowering of the coordination of the paramagnetic site will increase the energy gap between ground state and the first excited state as compared to higher coordinated sites, hence leading to a smaller deviation of the  $g_{\perp}$  value from the free electron value according to equation (1). When going from the edge center on a cube to an  $O^-$ -center at a monoatomic step, the  $g_{yy}$  and the  $g_{zz}$  component of the g-tensor show smaller values, while the value of the third component found close to the one of the free electron is unchanged ( $g_{xx}$ ). In this case the increase of the energy gap between ground state and first excited state qualitatively expected based on the experimental results is not readily explained by the change in the local coordination of the  $O^-$ -center. To gain some insight into the origin of the observed changes in the g-tensor components, it is interesting to look at the orientation of the g-tensor shown in the right side of Figure 7 for an  $O^-$ -center located at a step edge. The  $g_{xx}$ -component of the tensor is no longer found to be oriented close to the  $C_{2v}$ -axis of

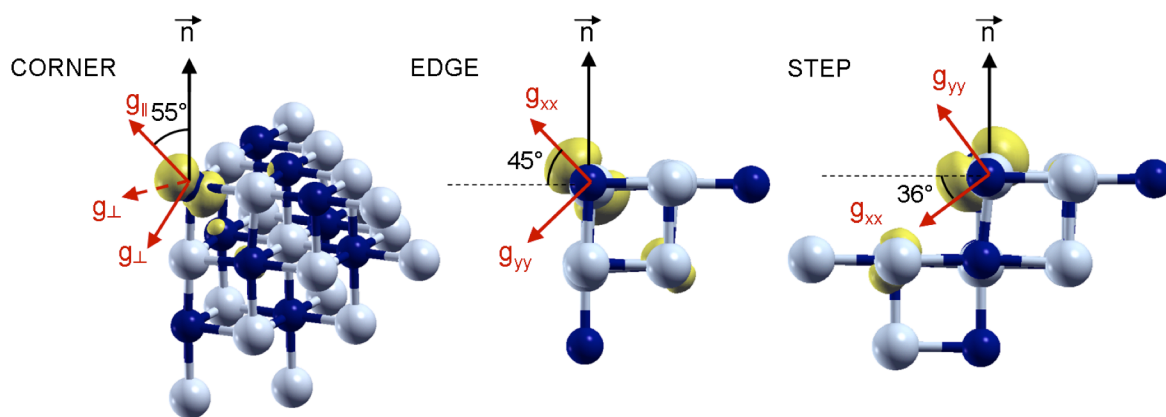


Figure 7: side view of a corner (left), an edge (center) and of a step edge (right) on a MgO(001) surface. Orientation of the three g-tensor components for the corner and of two g-tensor components in the plane perpendicular to the edge and step edge are shown with respect to the surface normal.

the edge site of the cube. It is rotated by  $81^\circ$  and exhibits an angle of  $36^\circ$  with respect to the upper terrace of the monoatomic step. As expected the spin density (shown in yellow) of the unpaired electron is found in a p-type orbital, which is oriented in the direction of the  $g_{xx}$ -component. A small fraction of the spin density is delocalized onto the adjacent oxygen anion on the lower terrace, which further stabilizes the trapped hole. The theoretically determined principal components of the g-tensor are in excellent agreement with the experimentally deduced ones. This is particularly worth noting as the deviations found for the description of g-tensor components of oxygen centered radicals on MgO surfaces are typically significantly larger. In particular, the high g-value component, which crucially depends on the proper description of the electronic structure (see introduction), is oftentimes described only semi-quantitatively (e.g. [9]). In addition, to the very good match of the principal components theory the rotation of the  $g_{xx}$ -component of the g-tensor towards the surface plane is found in the calculations, however, the orientation deduced from the experiment finds the  $g_{xx}$ -component closer to the surface ( $15^\circ$ ). Despite of the deviation in the orientation of the g-tensor between the experiment and theory, the

theoretical description of the  $O^-$ -center is very close to the experimentally observed results showing the level of agreement that can be reached if theory addresses well-defined model systems.

## **Conclusions**

In this study we have investigated the properties of  $O^-$ -centers on single-crystalline MgO(001) surfaces being created by the reaction of  $N_2O$  molecules with  $F^+$ -centers and discuss the coupling of these centers to Mo(V)-centers being located at the surface of these films. The  $F^+$ -centers were produced by electron bombardment of the MgO(001) films and were reported previously to be located predominantly the edges of the MgO islands. From angular dependent measurements it is possible to determine the orientation of the g-tensor for  $O^-$ -centers located at the edges of the MgO islands, which further confirms the assignment made for the  $F^+$ -centers. The g-tensor components calculated by ab-initio quantum chemistry of these centers are in quantitative agreement with the experiment. In addition, the theoretical treatment also reproduces the significant reorientation of the g-tensor with respect to the surface as compared to centers located on edges of MgO-cubes, which can be understood in terms of a different orientation of the O p-type orbital hosting the electron hole, pointing towards the closest lower terrace O anion for some electron delocalization. In addition to  $O^-$ -centers located on step edges the EPR results provide evidence for the presence of a minority species, which can be assigned to  $O^-$ -centers located at sites with a local symmetry plane expected for corner sites, which are known to be present as judged from the results of scanning probe experiments.

The analysis of the spectra obtained after filling the  $F^+$ -centers with atomic oxygen from  $N_2O$  at low temperature indicates that a fraction of about 30 % of the sites are subject to a subsequent electron transfer process from a reduced Mo(IV)-center. The latter reaction restores a

stoichiometric step edge and concomitantly oxidizes the Mo-center into an EPR active +V oxidation state, which is concluded from the reappearance of the signal already found on the pristine surface. Further annealing of such a sample to 300 K produces a new Mo-related signal at  $g = 1.985$ . This species can be assigned to Mo(V)-signals with a different coordination environment as compared to the pristine surface, which upon thermal treatment can be retransformed into the Mo(V)-centers found on the pristine film. This discussion provide some insight into the complex redox chemistry that is taking place on this well-defined single crystalline MgO(001) surface. It should be stressed at this point that transition metal doping is almost unavoidable for powdered oxide material and very serious efforts have to be taken to avoid doping on the tenth of ppm level. Hence, these effects may also be present in powdered materials used for high performance catalysis. In case the transition metal ion present as a dopant of the oxide can adopt different oxidation states a coupling of the redox chemistry of the doping centers with the intrinsic redox chemistry of the surface has to be taken into account to understand the properties of the system at hand.

#### **Acknowledgement**

A.G. and J.L. thank the IMPRS "Complex surfaces in Materials Science" for financial support. Valuable discussions with Martin Sterrer, Maxim Yulikov, Elio Giamello and Mario Chiesa are also gratefully acknowledged. Support was also provided from the Cluster of Excellence "Unifying Concepts in Catalysis" coordinated by Technische Universität Berlin and funded by the Deutsche Forschungsgemeinschaft. C.D.V. and G.P. thank the Italian MIUR for the FIRB Project No. RBAP115AYN, the Cariplo Foundation for the Grant No. 2013-0615, and the COST Action CM1104.

## References

1. Freund H-J, Goodman DW (2008) Ultrathin Oxide Films. In: Ertl G, Knözinger H, Schüth F, Weitkamp J (eds) Handbook of Heterogeneous Catalysis, vol 1. 2. edn. Wiley VCH, Weinheim, pp 1298-1309
2. Nilius N, Risse T, Schauer mann S, Shaikhutdinov S, Sterrer M, Freund HJ (2011) Model Studies in Catalysis. *Top Catal* 54 (1-4):4-12.
3. Pacchioni G, Freund H (2013) Electron Transfer at Oxide Surfaces. The MgO Paradigm: from Defects to Ultrathin Films. *Chem Rev* 113 (6):4035-4072.
4. Chiesa M, Giamello E, Che M (2010) EPR Characterization and Reactivity of Surface-Localized Inorganic Radicals and Radical Ions. *Chem Rev* 110 (3):1213-1808.
5. Yulikov M, Sterrer M, Heyde M, Rust HP, Risse T, Freund H-J, Pacchioni G, Scagnelli A (2006) Binding of single gold atoms on thin MgO(001) films. *Phys Rev Lett* 96 (14):146804.
6. Sterrer M, Fischbach E, Risse T, Freund H-J (2005) Geometric characterization of a singly charged oxygen vacancy on a single-crystalline MgO(001) film by electron paramagnetic resonance spectroscopy. *Phys Rev Lett* 94 (18):186101.
7. Chiesa M, Giamello E, Di Valentin C, Pacchioni G, Sojka Z, Van Doorslaer S (2005) Nature of the chemical bond between metal atoms and oxide surfaces: New evidences from spin density studies of K atoms on alkaline earth oxides. *J Am Chem Soc* 127 (48):16935-16944.
8. Livraghi S, Paganini MC, Giamello E, Selloni A, Di Valentin C, Pacchioni G (2006) Origin of Photoactivity of Nitrogen-Doped Titanium Dioxide under Visible Light. *J Am Chem Soc* 128 (49):15666-15671.

9. Gonchar A, Risse T, Freund H-J, Giordano L, Di Valentin C, Pacchioni G (2011) Activation of Oxygen on MgO:  $O_2^-$  Radical Ion Formation on Thin, Metal-Supported MgO(001) Films. *Angew Chem, Int Ed* 50 (11):2635-2638.
10. Weber H (1951) Die Verfärbung von MgO-Kristallen durch Gittereigene Bausteine. *Z Phys* 130 (3):392-402.
11. Nelson RL, Tench AJ, Harmsworth BJ (1967) Chemisorption on Some Alkaline Earth Oxides .1. Surface Centres and Fast Irreversible Oxygen Adsorption on Irradiated MgO, CaO and SrO. *Trans Faraday Soc* 63 (534P):1427.
12. Henderson B, Wertz JE (1968) Defects in the alkaline earth oxides. *Adv Phys* 17 (70):749-855.
13. Nelson RL, Tench AJ (1967) Chemisorption on Some Alkaline Earth Oxides .2. Intrinsic Bulk Defects and Adsorption of Oxygen on MgO CaO SrO. *Trans Faraday Soc* 63 (540P):3039.
14. Nelson RL, Hale JW, Harmsworth BJ, Tench AJ (1968) Surface Reactivity of Irradiated Magnesium Oxide - Effects of Dose on Defect Concentrations Specific Surface Areas and Chemisorption Kinetics. *Trans Faraday Soc* 64 (549P):2521-&.
15. Smith DR, Tench AJ (1968) Reaction of Hydrogen Atoms at Oxide Surfaces. *Chem Comm* (18):1113-&.
16. Tench AJ, Kibblewhite JFJ (1971) Electron Spin Resonance Study of Chlorine Radicals Stabilised on an Oxide Surface. *J Chem Soc A* (14):2282-&.
17. Tench AJ (1972) Oxygen Species Adsorbed on Oxides .2. Formation of (O-3)S on MgO. *J Chem Soc-Faraday Trans I* 68 (7):1181-&.
18. Zecchina A, Scarano D, Marchese L, Coluccia S, Giamello E (1988) Defect Centers on Mg-Doped MgO Surfaces. *Surf Sci* 194 (3):531-534.

19. Giamello E, Ferrero A, Coluccia S, Zecchina A (1991) Defect centers induced by evaporation of alkali and alkaline-earth metals on magnesium oxide: an EPR study. *J Phys Chem* 95 (23):9385-9391.
20. Giamello E, Murphy D (1994) Surface trapped electrons on metal vapour modified magnesium oxide. Nature of the surface centres and reactivity with adsorbed molecules. *Molecular Engineering* 4 (1):147-177.
21. Sterrer M, Diwald O, Knözinger E, Sushko PV, Shluger AL (2002) Energies and dynamics of photoinduced electron and hole processes on MgO powders. *J Phys Chem B* 106 (48):12478-12482.
22. Pinarello G, Pisani C, D'Ercole A, Chiesa M, Paganini MC, Giamello E, Diwald O (2001) O-radical ions on MgO as a tool to unravel structure and location of ionic vacancies at the surface of oxides: a coupled experimental and theoretical investigation. *Surf Sci* 494 (2):95-110.
23. Sterrer M, Diwald O, Knözinger E (2000) Vacancies and electron deficient surface anions on the surface of MgO nanoparticles. *J Phys Chem B* 104 (15):3601-3607.
24. Kramer J, Tegenkamp C, Pfnür H (2003) Formation of surface color centers at differently coordinated sites: MgO/Ag(1,1,19). *Phys Rev B* 67 (23):7.
25. Sterrer M, Heyde M, Novicki M, Nilus N, Risse T, Rust HP, Pacchioni G, Freund HJ (2006) Identification of color centers on MgO(001) thin films with scanning tunneling microscopy. *J Phys Chem B* 110 (1):46-49.
26. König T, Simon GH, Rust HP, Pacchioni G, Heyde M, Freund HJ (2009) Measuring the Charge State of Point Defects on MgO/Ag(001). *J Am Chem Soc* 131 (48):17544-17545.
27. Lunsford JH (1995) The Catalytic Oxidative Coupling of Methane. *Angew Chem, Int Ed* 34 (9):970-980.



28. Richter NA, Sicolo S, Levchenko SV, Sauer J, Scheffler M (2013) Concentration of Vacancies at Metal-Oxide Surfaces: Case Study of MgO(100). *Phys Rev Lett* 111 (4):045502.
29. McFarland EW, Metiu H (2013) Catalysis by Doped Oxides. *Chem Rev* 113 (6):4391-4427.
30. Sun XY, Li B, Metiu H (2013) Methane Dissociation on Li-, Na-, K-, and Cu-Doped Flat and Stepped CaO(001). *J Phys Chem C* 117 (14):7114-7122.
31. Arndt S, Laugel G, Levchenko S, Horn R, Baerns M, Scheffler M, Schlogl R, Schomacker R (2011) A Critical Assessment of Li/MgO-Based Catalysts for the Oxidative Coupling of Methane. *Catal Rev-Sci Eng* 53 (4):424-514.
32. Myrach P, Nilius N, Levchenko SV, Gonchar A, Risse T, Dinse KP, Boatner LA, Frandsen W, Horn R, Freund HJ, Schlögl R, Scheffler M (2010) Temperature-Dependent Morphology, Magnetic and Optical Properties of Li-Doped MgO. *Chemcatchem* 2 (7):854-862.
33. Dietl N, Schlangen M, Schwarz H (2012) Thermal Hydrogen-Atom Transfer from Methane: The Role of Radicals and Spin States in Oxo-Cluster Chemistry. *Angew Chem, Int Ed* 51 (23):5544-5555.
34. Schwach P, Willinger MG, Trunschke A, Schlögl R (2013) Methane Coupling over Magnesium Oxide: How Doping Can Work. *Angew Chem, Int Ed* 52 (43):11381-11384.
35. Tench AJ, Lawson T, Kibblewh.Jf (1972) Oxygen Species Adsorbed on Oxides. 1. Formation and Reactivity of (O-)S on MgO. *J Chem Soc-Faraday Trans I* 68 (7):1169-&.
36. Tench AJ, Lawson T (1970) The formation of O- and O adsorbed on an oxide surface. *Chem Phys Lett* 7 (4):459-460.
37. Wong NB, Lunsford JH (1971) Epr Study of O-17-on Magnesium Oxide. *J Chem Phys* 55 (6):3007-&.

38. Volkov AI (1986) Resonance Energy-Transfer from Solid to Adsorbed Molecules under Radiolysis of the N<sub>2</sub>O-MgO System. *J Chem Soc-Faraday Trans I* 82:815-829.
39. Di Valentin C, Ricci D, Pacchioni G, Chiesa M, Paganini MC, Giamello E (2002) O<sup>-</sup> radical anions on polycrystalline MgO. *Surf Sci* 521 (3):104-116.
40. Vannotti LE, Morton JR (1968) Paramagnetic-Resonance Spectra of S<sup>-</sup> Trapped in Alkali Halide Crystals. *Phys Rev* 174 (2):448-&.
41. Schmidt J, Risse T, Hamann H, Freund H-J (2002) Characterization of a model Ziegler-Natta catalyst for ethylene polymerization. *J Chem Phys* 116 (24):10861-10868.
42. Wu MC, Corneille JS, He JW, Estrada CA, Goodman DW (1992) Preparation, Characterization, and Chemical-Properties of Ultrathin MgO Films on Mo(100). *J Vac Sci Technol A* 10 (4):1467-1471.
43. Sterrer M, Fischbach E, Heyde M, Nilius N, Rust HP, Risse T, Freund H-J (2006) Electron paramagnetic resonance and scanning tunneling microscopy investigations on the formation of F<sup>+</sup> and F<sup>0</sup> color centers on the surface of thin MgO(001) films. *J Phys Chem B* 110 (17):8665-8669.
44. Stoll S, Schweiger A (2006) EasySpin, a comprehensive software package for spectral simulation and analysis in EPR. *J Mag Res* 178 (1):42-55.
45. Frisch MJ, Trucks GW, Schlegel HB, Scuseria GE, Robb MA, Cheeseman JR, Scalmani G, Barone V, Mennucci B, Petersson GA, Nakatsuji H, Caricato M, Li X, Hratchian HP, Izmaylov AF, Bloino J, Zheng G, Sonnenberg JL, Hada M, Ehara M, Toyota K, Fukuda R, Hasegawa J, Ishida M, Nakajima T, Honda Y, Kitao O, Nakai H, Vreven T, Montgomery Jr. JA, Peralta JE, Ogliaro F, Bearpark MJ, Heyd J, Brothers EN, Kudin KN, Staroverov VN, Kobayashi R, Normand J, Raghavachari K, Rendell AP, Burant JC, Iyengar SS, Tomasi J, Cossi M, Rega N, Millam NJ, Klene M, Knox JE, Cross JB, Bakken V, Adamo C, Jaramillo

J, Gomperts R, Stratmann RE, Yazyev O, Austin AJ, Cammi R, Pomelli C, Ochterski JW, Martin RL, Morokuma K, Zakrzewski VG, Voth GA, Salvador P, Dannenberg JJ, Dapprich S, Daniels AD, Farkas Ö, Foresman JB, Ortiz JV, Cioslowski J, Fox DJ (2009) Gaussian 09. Gaussian, Inc., Wallingford, CT, USA

46. Becke AD (1993) Density-functional thermochemistry. III. The role of exact exchange. *J Chem Phys* 98 (7):5648-5652.
47. Lee C, Yang W, Parr RG (1988) Development of the Colle-Salvetti correlation-energy formula into a functional of the electron density. *Phys Rev B* 37 (2):785 - 789.
48. Stevens WJ, Basch H, Krauss M (1984) Compact effective potentials and efficient shared-exponent basis sets for the first- and second-row atoms. *J Chem Phys* 81 (12):6026-6033.
49. Francl MM, Pietro WJ, Hehre WJ, Binkley JS, Gordon MS, DeFrees DJ, Pople JA (1982) Self-consistent molecular orbital methods. XXIII. A polarization-type basis set for second-row elements. *J Chem Phys* 77 (7):3654-3665.
50. Hehre WJ, Ditchfield R, Pople JA (1972) Self—Consistent Molecular Orbital Methods. XII. Further Extensions of Gaussian—Type Basis Sets for Use in Molecular Orbital Studies of Organic Molecules. *J Chem Phys* 56 (5):2257-2261.
51. Barone V (1996). In: Chong DP (ed) *Recent Advances in Density Functional Methods, Part I*. World Scientific, Singapur,
52. Neese F (2001) Prediction of electron paramagnetic resonance g values using coupled perturbed Hartree-Fock and Kohn-Sham theory. *J Chem Phys* 115 (24):11080-11096.
53. Tench AJ, Nelson RL (1968) Paramagnetic Defects Associated with Hydrogen Adsorbed on Surface of Magnesium and Calcium Oxides. *J Colloid Interface Sci* 26 (3):364-&.
54. Nelson RL, Tench AJ (1964) Chemisorption and Surface Defects in Irradiated Magnesium Oxide. *J Chem Phys* 40 (9):2736.

55. Giamello E, Murphy D, Ravera L, Coluccia S, Zecchina A (1994) Surface Color-Centers on Magnesium-Oxide Generated by Magnesium and Alkali-Metal Doping. *J Chem Soc-Faraday Trans 90* (20):3167-3174.
56. Chiesa M, Paganini MC, Giamello E, Di Valentin C, Pacchioni G (2003) First evidence of a single-ion electron trap at the surface of an ionic oxide. *Angew Chem, Int Ed* 42 (15):1759-1761.
57. Sterrer M, Berger T, Stankic S, Diwald O, Knözinger E (2004) Spectroscopic Properties of Trapped Electrons on the Surface of MgO Nanoparticles. *ChemPhysChem* 5 (11):1695-1703.
58. Sterrer M, Yulikov M, Fischbach E, Heyde M, Rust HP, Pacchioni G, Risse T, Freund HJ (2006) Interaction of gold clusters with color centers on MgO(001) films. *Angew Chem, Int Ed* 45 (16):2630-2632.
59. Schintke S, Messerli S, Pivetta M, Patthey F, Libioulle L, Stengel M, De Vita A, Schneider W-D (2001) Insulator at the Ultrathin Limit: MgO on Ag(001). *Phys Rev Lett* 87 (27):276801.
60. Gallagher MC, Fyfield MS, Bumm LA, Cowin JP, Joyce SA (2003) Structure of ultrathin MgO films on Mo(001). *Thin Solid Films* 445 (1):90-95.
61. Sousa C, Pacchioni G, Illas F (1999) Ab initio study of the optical transitions of F centers at low-coordinated sites of the MgO surface. *Surf Sci* 429 (1-3):217-228.
62. Sushko PV, Gavartin JL, Shluger AL (2002) Electronic properties of structural defects at the MgO (001) surface. *J Phys Chem B* 106 (9):2269-2276.
63. Scorza E, Birkenheuer U, Pisani C (1997) The oxygen vacancy at the surface and in bulk MgO: An embedded-cluster study. *J Chem Phys* 107 (22):9645-9658.

64. Ricci D, Di Valentin C, Pacchioni G, Sushko PV, Shluger AL, Giamello E (2003) Paramagnetic defect Centers at the MgO surface. An alternative model to oxygen vacancies. *J Am Chem Soc* 125 (3):738-747.
65. Di Valentin C, Neyman KM, Risse T, Sterrer M, Fischbach E, Freund H-J, Nasluzov VA, Pacchioni G, Rösch N (2006) Density-functional model cluster studies of EPR g tensors of F-s(+) centers on the surface of MgO. *J Chem Phys* 124 (4).
66. Gonchar A, Risse T (2013) Characterisation of paramagnetic Mo impurities on MgO(100) single-crystalline films grown on Mo(100). *Mol Phys* 111 (18-19):2708-2716.
67. Lian JC, Kieseritzky E, Gonchar A, Sterrer M, Rocker J, Gao HJ, Risse T (2010) N<sub>2</sub>O Adsorption on the Surface of MgO(001) Thin Films: An Infrared and TPD Study. *J Phys Chem C* 114 (7):3148-3151.
68. Sojka Z, Che M (1996) EPR investigation of the activation of N<sub>2</sub>O on Mo/SiO<sub>2</sub> catalysts via electron transfer: From N<sub>2</sub>O as a ligand to adsorbed O<sup>-</sup> ion. *J Phys Chem* 100 (35):14776-14785.
69. Lide DR (ed) (2005) Handbook of Chemistry and Physics. Handbook of Chemistry and Physics, 85 edn. CRC Press, Boca Raton
70. Diwald O, Sterrer M, Knözinger E, Sushko PV, Shluger AL (2002) Wavelength selective excitation of surface oxygen anions on highly dispersed MgO. *J Chem Phys* 116 (4):1707-1712.
71. Chiesa M, Giamello E, Di Valentin C, Pacchioni G (2005) The O-17 hyperfine structure of trapped holes photo generated at the surface of polycrystalline MgO. *Chem Phys Lett* 403 (1-3):124-128.
72. Hu Z, Li B, Sun X, Metiu H (2011) Chemistry of Doped Oxides: The Activation of Surface Oxygen and the Chemical Compensation Effect. *J Phys Chem C* 115 (7):3065-3074.

73. Di Valentin C, Pacchioni G (2014) Spectroscopic Properties of Doped and Defective Semiconducting Oxides from Hybrid Density Functional Calculations. *Acc Chem Res* 47 (11):3233-3241.
74. Nilius N, Freund H-J (2015) Activating Nonreducible Oxides via Doping. *Acc Chem Res* 48 (5):1532-1539.